A QSAR Model for in Silico Screening of MAO-A Inhibitors. Prediction, Synthesis, and Biological Assay of Novel Coumarins†

Lourdes Santana,*,‡ Eugenio Uriarte,‡ Humberto González-Díaz,‡,§ Giuseppe Zagotto,|| Ramón Soto-Otero,⊥ and Estefanía Méndez-Álvarez⊥

Department of Organic Chemistry, Faculty of Pharmacy, and Department of Biochemistry, Faculty of Medicine, University of Santiago de Compostela, 15872 Santiago de Compostela, Spain; Department of Pharmaceutical Sciences, University of Padova, 35131 Padova, Italy; and Department of Drug Design, Chemical Bio-actives Center, Central University of Las Villas, 54830 Santa Clara, Cuba

Received October 3, 2005

This work explores the potential of the MARCH-INSIDE methodology to seek a QSAR for MAO-A inhibitors from a heterogeneous series of compounds. A Markov model was used to quickly calculate the molecular electron delocalization, polarizability, refractivity, and *n*-octanol/water partition coefficients for a series of 1406 active/nonactive compounds. LDA was subsequently used to fit a classification function. The model showed 92.8% and 91.8% global accuracy and predictability in training and validation studies. This QSAR model was validated through a virtual screening of a series of coumarin derivatives. The 15 selected compounds were prepared and evaluated as in vitro MAO-A inhibitors. The theoretical prediction was compared with the experimental results and the model correctly predicted 13 compounds with only two mistakes on compounds with activities very close to the cutoff point established for the model. Consequently, this method represents a useful tool for the "in silico" screening of MAO-A inhibitors.

Introduction

Amine oxidases catalyze the oxidation of amines, diamines, and polyamines. Depending on their ability to preferentially recognize one of these substrates, amine oxidases can be divided into monoamine oxidases, diamine oxidases, and polyamine oxidases, respectively.[1,2] Several different enzymes fall into the amine oxidase class, and the classification of some of these systems still remains ambiguous. More specifically, monoamine oxidase (MAO) was the term introduced by Zeller in an attempt to distinguish one specific group of enzyme members of the class responsible for the oxidative deamination of monoamines.[3,4]

MAO exists in two isoforms (MAO-A and MAO-B), and each isoenzyme has a flavin adenine dinucleotide cofactor covalently linked to a cystein residue in the active center. Both MAO subtypes are characterized by specific substrates and inhibitors. MAO-A has a higher affinity for serotonin and norepinephrine, whereas MAO-B preferentially deaminates phenylethylamine and benzylamine. These properties determine the clinical importance of MAO inhibitors. Selective MAO-A inhibitors are used in the treatment of neurological disorders such as depression,[5,6] whereas the MAO-B inhibitors are useful in the treatment of Parkinson's[7] and Alzheimer's deseases.[8]

All of these aspects have led to an intensive search for novel MAO inhibitors (MAOIs), and this effort has increased considerably in recent years. Overall, three generations of MAOIs have been described. The first generation includes the irreversible and nonselective inhibitors. The second generation consists of all the irreversible but selective MAOIs. The discovery in the 1950s of the antidepressant properties of MAOIs was a major finding in the monoamine theory of depression. However, earlier MAOIs introduced into clinical practice were abandoned due to adverse effects, such as hepatotoxicity, orthostatic hypotension, and the so-called "cheese effect", which was characterized by hypertensive crisis. These drawbacks were thought to be related to nonselective and irreversible enzyme inhibition.[9,10]

In recent years, efforts have been focused on the discovery of reversible and selective MAOIs and this has led to a new class compounds (third generation). A broad consensus exists concerning the necessity for a search for novel MAOIs and the study of the mechanism of action for MAOs.[11,12] In any case, despite considerable progress in understanding the interactions of the two enzyme forms with their preferred substrates and inhibitors, few general rules are available for the rational design of potent and selective inhibitors.

It is clear that MAOs are tightly associated with the outer mitochondrial membrane; consequently, procedures to yield pure enzymes make use of detergents that are necessary to prevent aggregation or precipitation. For this reason, crystallization procedures are more difficult than for soluble proteins. This fact explains the research bottleneck in terms of obtaining detailed 3D structures of MAOs. Fortunately, the availability of large quantities of purified recombinant human MAOIs has provided suitable crystals for the elucidation of the structure of MAO-A[13] and MAO-B[14] isoforms. This in turn allowed accurate modeling of MAO inhibitors and opened new possibilities for the design of more selective drugs.

Moreover, once the 3D crystallographic structure of MAOs is resolved, the estimation of docking parameters for lead drug candidates may involve time-consuming operations where large libraries of chemicals must be investigated.

Consequently, novel approaches are also needed for the efficient search for new inhibitors, and although a number of reports exist on the quantitative structure−activity relationships (QSAR) for MAOIs, these are, in general, restricted to the study of congeneric families of compounds.[15]

† In memory of Prof. Cipriano Antonello.

* To whom correspondence should be addressed. Phone: +34-981-563100. Fax: +34-981 594912. E-mail: qolsant@usc.es.

‡ Department of Organic Chemistry, Faculty of Pharmacy, University of Santiago de Compostela.

§ Central University of Las Villas.

|| Department of Biochemistry, Faculty of Medicine, University of Santiago de Compostela.

⊥ University of Padova.

10.1021/jm0509849 CCC: $33.50
Published on Web 12/21/2005

In this sense, the development of QSARs using simple molecular indices appears to be a promising alternative or complementary technique to drug−protein docking, high-throughput screening, and combinatorial chemistry techniques. Almost all QSAR techniques are based on the use of molecular descriptors, which are numerical series that codify useful chemical information and enable correlations between statistical and biological properties.[16−18]

A large number of examples have been published in which the use of molecular descriptors has become a rational alternative to massive synthesis and screening of compounds in medicinal chemistry.[19,20] Indeed, experience has shown that the use of models fitted with large data sets of chemicals works as well as the use of models built from a series of homologous compounds and is also a more general method that can be applied in a broad spectrum of cases. The principal deficiency in the use of some molecular indices concerns their lack of physical meaning. In this respect, the introduction of novel molecular indices must obey physicochemical laws in order to ensure a theoretically rigorous interpretation of the results.[18]

In the particular case of MAOIs, electron delocalization and its consequences—such as polarizability and hydrophobicity—may be a determinant physical factor. This issue can be explained by considering that two models have been proposed for MAO catalysis and these involve an electron transfer or polar nucleophilic mechanisms.[11,14]

Quantum chemical calculations can be used to obtain a priori descriptors for QSAR studies. Given that some of these quantum properties are not observable, the best way to calculate them is not uniquely defined. Consequently, it is likely that there are many different schemes for such calculations, and none of these is fundamentally more correct than another. Unfortunately, the calculations are often also computationally too demanding for large sets of molecules.[21] In an effort to address this difficulty, Bultinck et al.[22] described the implementation of a computational approach based on the electronegativity equalization principle (EEP) to allow the very rapid calculation of atomic charges and related molecular descriptors. According to the EEP described by Sanderson, when molecules are formed, the electronegativities and other properties of the constituent atoms become equal, coinciding with a fixed distribution for probabilities of finding the electrons in the neighborhood of a specific atom in the molecule at the steady state.[23,24] Simpler and faster methods to calculate molecular descriptors based on the idea of EEP are of interest in terms of their application to very large databases of compounds with the aim of finding druglike leads.

Our research group has just introduced a novel series of stochastic indices in the so-called MARCH-INSIDE approach. The method is based on the use of Markov models (MM)[25] to codify useful chemical structure information in terms of molecular electron delocalization, polarizability, refractivity, and *n*-octanol/water partition coefficient.[26−28]

In this work we will explore the potential of MARCH-INSIDE to seek a QSAR for MAO-A inhibitors from a heterogeneous series of compounds. In the first step, the aforementioned molecular descriptors were calculated for a large series of active/nonactive compounds. Linear discriminant analysis (LDA) was subsequently used to fit a classification function. The QSAR developed was then validated with an external predicting series by the resubstitution technique. Finally, the model was used for the prediction of a novel generation of MAO-A inhibitors, which were subsequently synthesized, structurally characterized, and experimentally assayed.

Results and Discussion

Computational Methods. The MARCH-INSIDE approach (*Mar*kovian *ch*emicals *in si*lico *de*sign) is based on the calculation of the different physicochemical molecular properties as an average of atomic properties (ap). For instance, it is possible to derive average estimations of molecular or group electronegativities [$^k\chi(G)$], refractivities [^{k}MR(G)], polarizabilities [$^k\alpha(G)$], and logarithms of water/*n*-octanol partition coefficients (log ^kP).

$$^k\chi(G) = \sum_{j \in G} p_k(\chi_j)\, \chi_j \tag{1}$$

$$^k\mathrm{MR}(G) = \sum_{j \in G} p_k(\mathrm{MR}_j)\, \mathrm{MR}_j \tag{2}$$

$$^k\alpha(G) = \sum_{j \in G} p_k(\alpha_j)\, \alpha_j \tag{3}$$

$$\log {}^kP(G) = \sum_{j \in G} p_k(\log P_j) \log P_j \tag{4}$$

It is possible to consider isolated atoms ($k = 0$) in the estimation of the molecular properties $^0\chi(G)$, ^{0}MR(G), $^0\alpha(G)$, log ^0P. In this case the probabilities $^0p(ap_j)$ are determined without considering the formation of chemical bonds (simple additive scheme). However, it is possible to consider the gradual effects of the neighboring atoms at different distances in the molecular backbone. To achieve this goal, the method uses a MM, which determines the absolute probabilities $p_k(ap_j)$ with which the atoms placed at different distances k affect the contribution of the atom j to the molecular property in question. For example, in the case of molecular polarizability

$$^k\alpha = [p(\alpha_1)p_0(\alpha_2)...p_0(\alpha_n)]\cdot \begin{bmatrix} {}^1p_{1,1} & {}^1p_{1,2} & {}^1p_{1,3} & \cdot & {}^1p_{1,n} \\ {}^1p_{2,1} & {}^1p_{2,2} & {}^1p_{2,3} & \cdot & {}^1p_{2,n} \\ \cdot & \cdot & \cdot & \cdot & \cdot \\ \cdot & \cdot & \cdot & \cdot & \cdot \\ {}^1p_{n,1} & \cdot & \cdot & \cdot & {}^1p_{n,n} \end{bmatrix}^k \cdot \begin{bmatrix} \alpha_1 \\ \alpha_2 \\ \cdot \\ \cdot \\ \alpha_n \end{bmatrix} = \sum_{j=1}^{n} p_k(\alpha_j)\, \alpha_j$$

From left to right, the first term is $^k\alpha$, which is the average molecular polarizability of the molecule considering the effects of all the atoms placed at distance k over every atomic polarizability α_j. The vector on the left-hand side of the equation contains the probabilities $^0p(\alpha_j)$ for every atom in the molecule, without considering chemical bonds. The matrix in the center of the equation is the so-called stochastic matrix. The values of this matrix ($^1p_{ij}$) are the probabilities with which every atom affects the polarizability of the atom bonded to it. Both kinds of probabilities $^0p(\alpha_j)$ and $^1p_{ij}$ are easily calculated from atomic polarizabilities (α_j) and the chemical bonding information:

$$^0p_{ij} = \frac{\alpha_j}{\sum_{k=1}^{n} \alpha_k} \tag{6}$$

$$^1p_{ij} = \frac{\delta_{ij}\alpha_j}{\sum_{k=1}^{n} \delta_{ik}\alpha_k} \tag{7}$$

The only difference is that in the probabilities $^0p(\alpha_j)$ we consider

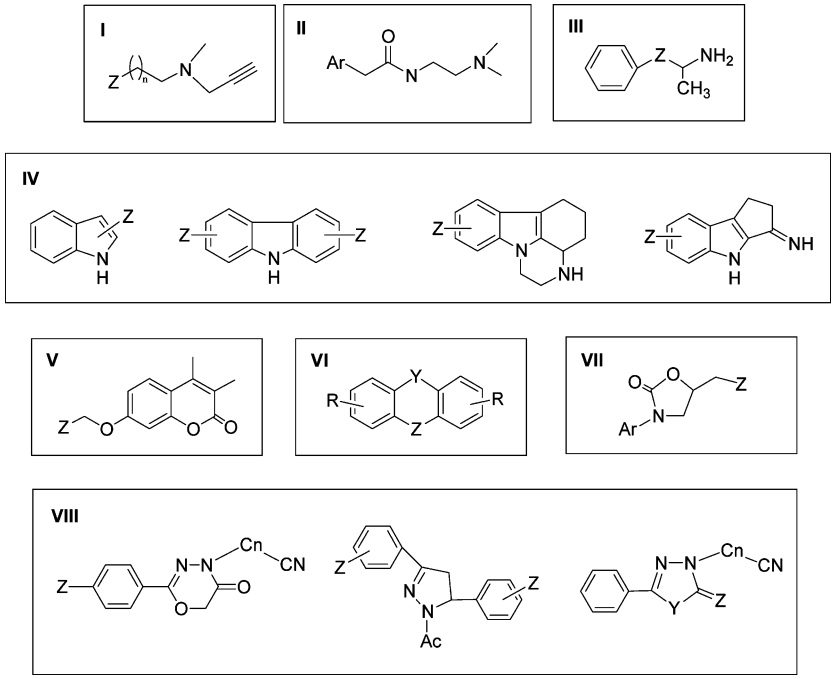

Figure 1. Structural sets of known MAO-A inhibitors used in the QSAR study.

isolated atoms by carrying out the sum in the denominator over all n atoms in the molecule. On the other hand, for $^1p_{ij}$, chemical bonding is taken into consideration by means of the factor δ_{ij}. This factor has a value of 1 if atoms i and j are chemically bonded and is 0 otherwise.

Finally, it is interesting to note that one can sum only the atoms included in a specific group (G) rather than all atoms. In this way, we can approach specific classes of average properties such as the average electronegativity for sp_3 carbon atoms (C_{sp3}) or average polarizability for heteroatoms (Het). All calculations were performed using the program MARCH-INSIDE,[28] which was developed in-house.

General QSAR for MAO-A Inhibitors. The development of a discriminant function[29] that allows the classification of organic compounds as active or inactive is the key step in the present approach for the discovery of MAO-A inhibitors. It was therefore necessary to select a training data set of MAO-A inhibitors containing wide structural variability. Here we consider a general data set of 1406 compounds, 674 of which have MAO-A inhibitory activity. This group contains chemicals with IC_{50} values ≤ 25 μM or in some cases compounds that show an inhibition percentage of $\geq 50\%$ at inhibitor concentrations ≤ 25 μM. This series is composed at random of the most representative families of MAO-A inhibitors taken from the literature (Supporting Information); these include propargyl (clorgyline analogues) (**I**), benzamide (moclobemide analogues) (**II**), phenylethylamine (**III**), indole (**IV**), coumarin (**V**), thioxanthene (**VI**), oxadiazolidone (toloxatone analogues) (**VII**), and diazoheterocyclic derivatives (**VIII**) (see Figure 1).

The remaining 732 compounds were a heterogeneous series of inactive compounds, including members of the aforementioned families, with $IC_{50} > 25$ μM, along with many other structural patterns extracted from international databases.[30,31] It is common for compounds with even higher IC_{50} values to be considered as active or moderately active, but we considered 25 μM to be a reasonable limit. The selection of higher break point values to cluster chemicals by their MAO-A IC_{50} may generate a series with a clearly disproportionate size and, therefore, a vastly reduced number of active compounds. The selection here of discriminant techniques instead of regression techniques was determined by the lack of homogeneity in the conditions under which these values were measured. As reported in different sources, numerous IC_{50} values lie within a range rather than a single value. In other cases, the activities are not scored in terms of IC_{50} values but are quoted as inhibitory percentages at a given concentration. Once the training series had been designed, forward stepwise linear discriminant analysis (LDA) was carried out in order to derive the QSAR for the MAO-A inhibitory activity score (i-MAO-A):

$$\text{i-MAO-A} = -1.32\chi_1(C_{sat}) - 2.56\chi_2(\text{Het}) + 0.46\alpha_0(\text{Het}) + 1.69\alpha_1(\text{Het}) + 1.16MR_1 + 7.12MR_2(C_{unsat}) - 1.71MR_0(\text{Het}) - 2.95\cdot\log P_0 - 5.6\cdot\log P_2(C_{unsat}) + 1.21$$

$$\lambda = 0.36 \quad F = 273.93 \quad p < 0.01$$

The statistical significance of this model was determined by examining Wilk's λ statistic, the Fisher ratio (F), and the p-level (p). We also inspected the percentage of good classification in training and validation experiments. LDA produced a classification function that gave rise to an efficient separation of 92.8% of the 1406 chemicals (training series) into two groups. The model correctly classified 95.1% of 674 MAO-A inhibitors and 90.73% of the 732 inactive compounds. This is equivalent to predicting the inhibitory probability of 641 MAO-A inhibitors out of 674 and 664 inactive chemicals out of 732 (see Table 1).

Validation of the model was carried out by the resubstitution approach. In this kind of validation technique the data set is first split into one training subset and a predicting subset or control series. Next, the model is derived again using only the compounds in the training subset. In the third step, the compounds in both the training and predicting subsets (not used to seek the new model) are classified. The compounds in the training and predicting subsets are then interchanged at random several times (10 times in this case). Finally, the average predictability for all of the interchanged series is reported. In this study the model presented an average validation predict-

Table 1. Training and Validation Results

	percent	MAO-A inhibitors	nonactive	total
	Training Results			
MAO-A inhibitors	95.1	641	33	674
nonactive	90.7	68	664	732
total	92.8			1406
	Validation Results			
MAO-A inhibitors	93.6	631	43	674
nonactive	90.1	72	660	732
total	91.8			1406

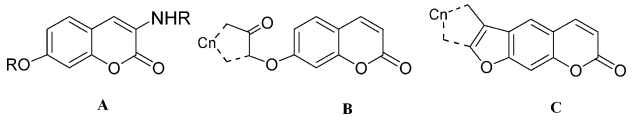

Figure 2.

ability of 91.8%. This result shows that the model not only has a high predictability but also a high robustness to data variation (see Table 1). The names, observed classification, predicted classification, and subsequent probabilities for all 1406 compounds in training and average validation are given as Supporting Information.

The in Silico Evaluation of Novel MAO-A Inhibitors. The model developed in this study was used for the design of novel MAO-A inhibitors. As described previously, a specific way to new lead discovery involves several general common steps when it is used in terms of a QSAR: (a) construction of a suitable molecular database of compounds that either show MAO-A inhibitory activity or do not, (b) calculation of the molecular descriptors, (c) construction of the model, (d) estimation of the biological activity using QSAR, (e) synthesis and characterization of selected compounds, and (f) assay of the candidate compounds in order to corroborate the predicted biological activity.

As mentioned above, the coumarin analogues are a family of natural and/or synthetic compounds with different pharmacological activities,[32] one of which is MAO inhibitory activity.[33−35] In many cases, it is know that activity and selectivity are determined by the nature of the substituent in position 7 (**V** structural set in Figure 1).[33,34] On the other hand, the influence on MAO-A activity of amino groups in position 3 of coumarins (**A** analogues), as well as the furocoumarins (**B** analogues) and tetracyclic coumarin derivatives (**C** analogues), has not been explored in this field (Figure 2).

On the basis of the above information, and considering our experience with this family of compounds, we designed and calculated the molecular descriptors for new coumarin analogues.

The designed compounds were evaluated by the QSAR model. We selected 15 coumarin derivatives with different levels of structural complexity and, of these, 11 were determined as active and 4 as inactive.

Synthesis. Compound **1** (8-MOP) is commercially available and compounds **2**, **3**, **5**−**9**, **11**, **12**, **14**, **16**, **18**, **20**, and **24** were efficiently synthesized according to Schemes 1−5. Compounds **2** and **3** were obtained from 8-MOP by following three-step synthetic routes[35−37] (Scheme 1). Reaction of 7-hydroxy-4-methylcoumarin (**4**) with 2-chlorocyclohexanone or 2-chlorocyclopentanone under Williamson conditions gave compounds **5** and **8**, respectively.[38−40] These compounds were treated with alkali to give compounds **6** and **9**. Finally, compound **6** was oxidized with DDQ to give benzofurocoumarin **7**[38] (Scheme 2). Compounds **11** and **12** were obtained from 5-methoxy-

Scheme 1[a]

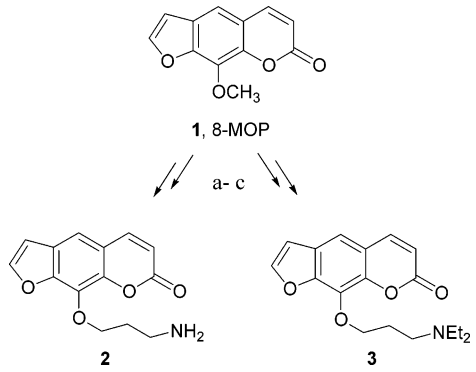

[a] Reagents and conditions: (a) $AlCl_3/CH_2Cl_2$, rt; (b) $Br(CH_2)_3$ Br/K_2CO_3, acetone, reflux; (c) potassium phthalimide/DMA, rt then $CH_3NHNH_2/CHCl_3$, rt for **2**; Et_2NH/EtOH, 65 °C for **3**.

Scheme 2[a]

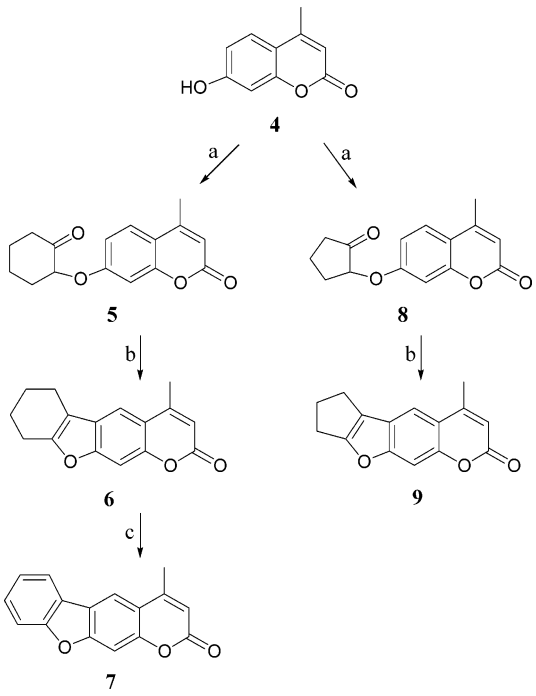

[a] Reagents and conditions: (a) 2-chlorocycloalkanone/K_2CO_3, acetone, reflux; (b) 0.1 N NaOH, reflux; (c) DDQ, toulene, reflux.

resorcinol (**10**) through 7-hydroxy-5-methoxy-4-methylcoumarin and 5-hydroxy-7-methoxy-4-methylcoumarin, respectively.[39−41] In a similar way compound **14** was obtained from 2-methoxyresorcinol (**13**)[42] (Scheme 3). Compound **16**[43] was prepared from 2,4-dihydroxy-3-methoxybenzaldehyde (**15**) and was *N*-acetylated and treated with chloroacetone under Williamson conditions to give compound **18** in 60% overall yield. Treatment of **18** in a strong alkaline medium led to the furan ring, and subsequent hydrolysis of the amide group in an acidic medium afforded furocoumarin **20** in 63% overall yield (Scheme 4). 3-Aminofurocoumarin **21**[44] was used to synthesize the corresponding *N*-glycyl derivative **24** according to Scheme 5. *N*-Acetylation of **21** with bromoacetyl chloride, subsequent replacement of the bromo substituent by a phthalimide group, and hydrolysis of the imide gave **24** in 45% overall yield.

MAO-A Inhibition Assay. The synthesized compounds were tested for their inhibitory effect on MAO-A. The inhibition data (expressed as IC_{50} values) are reported in Table 2. Compound **8** showed the highest activity, with an IC_{50} value of 0.04 μM. The three analogues **3**, **12**, and **16** did not inhibit MAO-A even

Scheme 3[a]

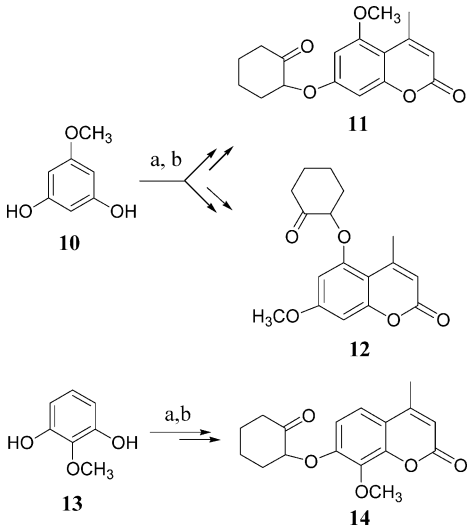

[a] Reagents and conditions: (a) $CH_3COCH_2CO_2Et/H_2SO_4$, 25 °C; (b) 2-chlorocyclohexanone/K_2CO_3, acetone, reflux.

Scheme 4[a]

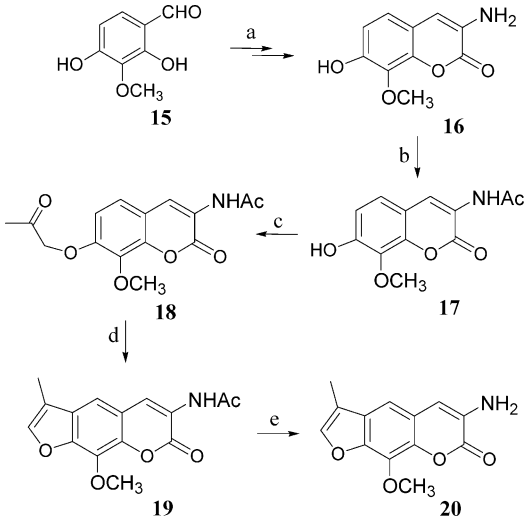

[a] Reagents and conditions: (a) $NH_2CH_2CO_2H/Ac_2O/Ac_2ONa$, reflux; 3 N HCl; (b) Ac_2O/Ac_2OH, 0 °C; (c) $ClCH_2COCH_3/K_2CO_3$/acetone, reflux; (d) 0.1 M NaOH/EtOH, reflux; (e) (i) 3 M HCl/MeOH, reflux; (ii) $NaHCO_3$.

at the highest concentration tested (200 μM). Three other compounds (**1**, **5**, and **6**) showed moderate activity, with IC_{50} values in the range 43−85 μM. All of the other assayed compounds had IC_{50} values in the range 0.04−22 μM.

To further investigate the MAO-A inhibition mechanism, the most potent inhibitor (**8**) was selected. The inhibition of MAO-A by this compound (a sigmoid function) provided evidence for the existence of reversible inhibition (Figure 3A). Kinetic analysis was carried out using Lineweaver−Burk plots. The inset (Figure 3B) shows the secondary plot of slope versus the concentration of **8**. The data indicate a noncompetitive inhibition mechanism.

Conclusions

A total of 11 compounds were predicted to be active in the in silico evaluation carried out using the QSAR model developed here; compounds were considered active when they had an IC_{50} value below 25 μM. Of these compounds, a total of nine were confirmed to be active by in vitro tests, and one of these compounds (**8**) had a very high activity. Two compounds that were predicted as active (compounds **5** and **6**) were found to have IC_{50} values of 43.0 and 65.2 μM, respectively, and although these compounds are considered inactive by our cutoff point, the values are in the range often considered as active. 8-MOP (compound **1**) and compounds **3**, **12**, and **16** were predicted to be inactive by the model, and the experimental data agree with this classification, even at the highest concentration tested (200 μM).

In conclusion, in the work described here, we developed a MARCH-INSIDE methodology that allowed us to predict by in silico screening the in vitro inhibitory MAO-A activity in a rapid and efficient way. In addition, the significance of this approach is that a QSAR model for the MAO inhibitors was able to correctly classify, for the first time, a series of compounds with different structural patterns. This ability demonstrates that this is a general model and we can therefore conclude that the MARCH-INSIDE approach represents a promising tool for the discovery of active compounds as drugs.

Scheme 5[a]

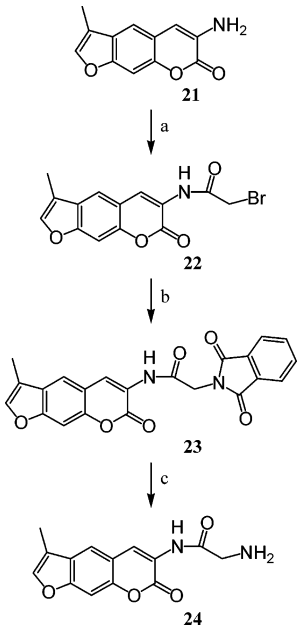

[a] Reagents and conditions: (a) $BrCH_2COCl$/pyridine/toulene, rt; (b) potassium phthalimide/DMA, rt; (c) $CH_3NHNH_2/CHCl_3$, rt.

Table 2. In Silico and in Vitro Evaluation of MAO-A Inhibition of Selected Compounds

		G[a]		
compd	IC_{50} (μM)	observed	predicted	p[b] active (%)
2	2.51	+	+	96.13
7	7.24	+	+	99.86
8	0.04	+	+	99.04
9	11.90	+	+	99.75
11	21.41	+	+	98.61
14	11.13	+	+	98.51
18	6.43	+	+	95.16
20	21.74	+	+	95.98
24	12.35	+	+	88.34
5	43.02	−	+	99.00
6	65.25	−	+	99.75
1	85.11	−	−	12.5
3	>200	−	−	0.45
12	>200	−	−	1.39
16	>200	−	−	42.30

[a] The observed and predicted groups for the selected compounds; −, a given compound lies within the group; +, the $IC_{50} < 25$ μM for the observed group and $p > 50\%$ for predicted group. [b] p is the subsequent probability predicted by the model.

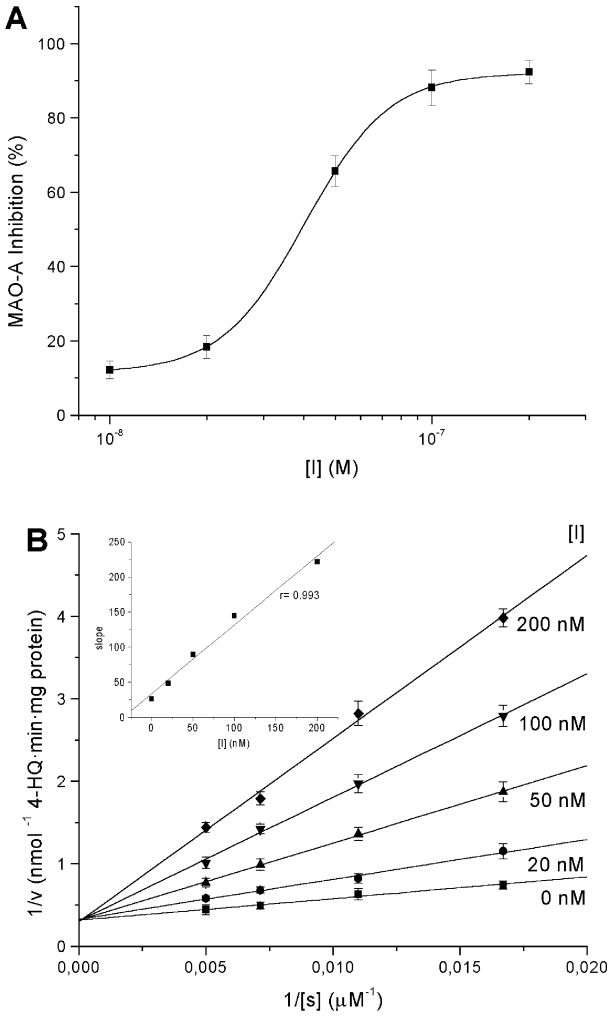

Figure 3. (A) Inhibition of MAO-A by compound **8**. Each point represents mean ± SEM from triplicate determinations. (B) Lineweaver−Burk plots and secondary replot of MAO-A inhibition by **8** showing a linear competitive mechanism. All values represent mean ± SEM from triplicate determinations.

Experimental Section

Chemistry. Melting points were determined using a Reichert Kofler thermopan or in capillary tubes on a Büchi 510 apparatus and are uncorrected. IR spectra were recorded on a Perkin-Elmer 1640FT spectrophotometer. ^{1}H and ^{13}C NMR spectra were recorded on a Bruker AMX spectrometer at 300 and 75.47 MHz, respectively, using TMS as internal standard (chemical shifts in δ values, J in hertz). Mass spectra were obtained using a Hewlett-Packard 5988A spectrometer. Elemental analyses were performed using a Perkin-Elmer 240B microanalyzer and were within ±0.4% of calculated values in all cases. Silica gel (Merck 60, 230−00 mesh) was used for flash chromatography (FC). Analytical thin-layer chromatography (TLC) was performed on plates precoated with silica gel (Merck 60 F254, 0.25 mm).

3-Acetylamino-7-hydroxy-8-methoxycoumarin (17). To a solution of compound **16**[43](2 g, 9.66 mmol) in 30% acetic acid (250 mL) at 0 °C was added acetic anhydride (5 mL, 52.94 mmol). The resulting precipitate was filtered off to give **17**: yield 2.04 g (85%); mp 228 °C; ^{1}H NMR (DMSO-d_6) 10.25 (bs, 1H, HO), 9.68 (s, 1H, HN), 8.50 (s, 1H, H-4), 7.26 (d, 1H, H-5, J = 8.5), 6.86 (d, 1H, H-6, J = 8.5), 3.83 (s, 3H, CH_3O), 2.13 (s, 3H, CH_3CO); IR 3324, 2990, 2975, 1708, 1670, 1603, 1544, 1237. Anal. ($C_{12}H_{11}NO_5$) C, H, N.

7-Acetonyloxy-3-acetylamino-8-methoxycoumarin (18). To a solution of **17** (1 g, 4.01 mmol) in dry acetone (300 mL) were added K_2CO_3 (4 g) and chloroacetone (1 mL, 12.6 mmol). The reaction mixture was heated under reflux for 20 h. The precipitate was filtered off, the organic phase was concentrated to dryness, and the residue was purified by FC using 1:1 toluene/ethyl acetate as eluent to give **18**: yield 860 mg (70.5%); mp 207 °C; ^{1}H NMR ($CDCl_3$) 8.62 (s, 1H, H-4), 8.00 (bs, 1H, HN), 7.17 (d, 1H, H-5, J = 8.5), 6.75 (d, 1H, H-6, J = 8.5), 4.69 (s, 2H, CH_2), 4.04 (s, 3H, CH_3O), 2.32 and 2.24 [2s, 3 + 3H, 2(CH_3O)]; IR 3325, 3110, 2944, 1713, 1674, 1605, 1538, 1140. Anal. ($C_{15}H_{15}NO_6$) C, H, N.

3-Acetylamino-8-methoxy-4′-methylfuro[3,2-*g*]coumarin (19). To a solution of **18** (1 g, 3.39 mmol) in ethyl alcohol (200 mL) was added 0.1 M NaOH (200 mL). The mixture was heated under reflux for 3 h, acidified with HCl, concentrated to half-volume, and left overnight. The resulting precipitate was filtered off and purified by FC using 9:1 toluene/ethyl acetate as eluent to give **19**: yield 620 mg (66%); mp 248−249 °C; ^{1}H NMR ($CDCl_3$) 8.77 (s, 1H, H-4), 8.05 (bs, 1H, HN), 7.47 (d, 1H, H-5′, J = 1.3), 7.28 (s, 1H, H-5), 4.32 (s, 3H, CH_3O), 2.26 (d, 3H, CH_3, J = 1.3), 2.25 (s, 3H, CH_3CO); IR 3329, 3110, 2954, 1711, 1677, 1594, 1531, 1389, 1142. Anal.($C_{15}H_{13}NO_5$) C, H, N.

3-Amino-8-methoxy-4′-methylfuro[3,2-*g*]coumarin (20). A mixture of **19** (500 mg, 1.74 mmol), methyl alcohol (150 mL), and 3 M HCl (75 mL) was heated under reflux for 1 h. The mixture was allowed to cool and was neutralized with $NaHCO_3$ and concentrated to 30% of its initial volume. The precipitate was filtered off to give **20**: yield 409 mg (96%); mp 139−140 °C; ^{1}H NMR ($CDCl_3$) 7.43 (d, 1H, H-5′, J = 1.3), 7.04 (s, 1H, H-5), 6.81 (s, 1H, H-4), 4.28 (s, 3H, CH_3O), 2.24 (d, 3H, CH_3, J = 1.3); IR 3324, 3110, 2947, 1707, 1638, 1577, 1352, 1169, 1087, 766. Anal. ($C_{13}H_{11}NO_4$) C, H, N.

3-Bromoacetylamino-4′-methylfuro[3,2-*g*]coumarin (22). To a solution of 3-amino-4′-methylfuro[3,2-*g*]coumarin[44] (**21**, 500 mg, 2.32 mmol) in toluene (200 mL) was added pyridine (0.2 mL, 2.47 mmol) and bromoacetyl chloride (1 mL, 12.10 mmol). The mixture was stirred for 1 h at room temperature. The resulting precipitate was filtered off and the solution evaporated under vacuum to give **22**: yield 632 mg (80%); mp 215−217 °C; ^{1}H NMR ($CDCl_3$) 8.90 (bs, 1H, HN), 8.81 (s, 1H, H-4), 7.64 (s, 1H, H-5), 7.49 (d, 1H, H-5′, J = 1.3), 7.45 (s, 1H, H-8), 4.04 (s, 2H, CH_2), 2.28 (d, 3H, CH_3, J = 1.3); IR 3309, 1707, 1673, 1542, 1362, 1161. Anal. ($C_{14}H_{10}BrNO_4$) C, H, N.

3-Phthalylacetamido-4′-methylfuro[3,2-*g*]coumarin (23). To a solution of potassium phthalimide (350 mg, 1.90 mmol) in dimethylacetamide (20 mL) was added bromo derivative **22** (500 mg, 1.48 mmol). The mixture was stirred for 4 h at room temperature, acetic acid (2 mL) was added, and the mixture was left overnight at 0 °C. The resulting precipitate was filtered off and washed with toluene to give **23**: yield 512 mg (85.6%); mp 312 °C; ^{1}H NMR (DMSO-d_6) 10.37 (s, 1H, HN), 8.69 (s, 1H, H-4), 8.00−7.85 (m, 6H, H-5 + H-5′ + phthalimide), 7.70 (s, 1H, H-8), 4.63 (s, 2H, CH_2), 2.22 (s, 3H, CH_3); IR 3341, 1725, 1710, 1688, 1532, 1420, 1200, 1147. Anal. ($C_{22}H_{14}N_2O_6$) C, H, N.

3-Aminoacetamido-4′-methylfuro[3,2-*g*]coumarin (24). A mixture of phthalimido derivative **23** (500 mg, 1.24 mmol), methyl hydrazine (0.5 mL, 9.35 mmol), HCl_3 (12 mL), and ethyl alcohol (12 mL) was stirred for 6 h at room temperature. The solvent was evaporated under vacuum and the residue washed with hexane and recrystallized from ethyl alcohol to give **24**: yield 225 mg (66.5%); mp 291−293 °C; ^{1}H NMR (DMSO-d_6) 8.75 (s, 1H, H-4), 8.01 (s, 1H, H-5), 7.88 (d, 1H, H-5′, J = 1.1), 7.69 (s, 1H, H-8), 3.91 (s, 2H, CH_2), 2.26 (d, 3H, CH_3, J = 1.1); IR 3245 1711, 1663, 1626, 1540, 1458, 1447, 1141. Anal. ($C_{14}H_{12}N_2O_4$) C, H, N.

Animals and Brain Mitochondria Preparations. Adult male Sprague−Dawley rats weighing 200−250 g were used. The rats were anesthetized with carbon dioxide and killed by decapitation. The brains were removed in an ice-cold isolation medium containing 0.32 M sucrose, 10 mM Tris-HCl buffer, pH 7.4. Blood vessels and pial membranes were removed and mitochondria were then prepared according to a previously published method.[45]

Determination of MAO-A Activity. MAO-A activity was determined spectrophotometrically according to a previously reported method.[41] Mitochondrial incubations (final protein concen-

tration 1 mg/mL) were performed in 100 mM potassium phosphate buffer (pH 7.4) at 37 °C. The mitochondria were preincubated at 37 °C for 5 min with the selective irreversible MAO-A inhibitor clorgyline (250 nM). After a second preincubation with DMSO (control) or the potential inhibitor dissolved in DMSO, the nonselective substrate kynuramine was added at a concentration equal to its K_M (90 μM for MAO-A). The final DMSO concentration was 5% (v/v). The formation of 4-hydroxyquinoline was continuously monitored at 314 nm.

For each inhibitor, IC_{50} values were determined from MAO-A inhibition/−log concentrations plots, using the graph package Origin v. 6.0 (Microcal Software Inc., Northampton, MA). Analysis of the corresponding Lineweaver−Burk plots enabled the mechanism of the inhibition to be assessed.

The reversibility of the inhibition was assessed by dialysis, as reported previously.[46] Briefly, the procedure involved incubation of mitochondria preparations (1 mg/mL) containing clorgyline (250 nM) at 37 °C for 15 min in the absence (control) or presence of the inhibitor concentration equal to its IC_{50}. These mixtures were then dialyzed using a Biodialyzer (Sigma Chemical Co.) with an ultrafiltration membrane of nominal molecular weight limit 10 000. The dialysis was preformed at 4 °C using 250 mL of outer buffer (100 mM potassium phosphate buffer, pH 7.4). The outer buffer was replaced with fresh buffer every 30 min for a period of 2 h. Dialyzed mixtures were then assayed for MAO-A activity.

Computer Software. The calculation of the molecular descriptors was implemented in the in-house software MARCH-INSIDE. This software has a graphical interface that makes it user-friendly for medicinal chemists.

Acknowledgment. We are grateful to the Xunta de Galicia (PGIDIT02BTF20301PR and PGIDIT05BTF20302PR2) for partial financial support. The authors would like to acknowledge the referees for useful comments, which have undoubtedly improved the final presentation of the manuscript.

Supporting Information Available: Elemental analyses data for synthesized compounds; bibliographic references for database compounds; Table 3, a complete list of compounds used in training sets with the indication of the compound number in the corresponding bibliographic reference as well as their observed classification, predicted classification, training, and subsequent validation probabilities; and Table 4, a list of values of the molecular descriptors contained in the model. This material is available free of charge via the Internet at http://pubs.acs.org.

References

(1) Dostert, P.; Strolin Benedetti, M.; Jafre, M. *Monoamine Oxidase: Basic and Clinical Frontiers;* Elsevier: Amsterdan, 1982.
(2) Singer, T. P. In *Chemistry and Biochemistry of Flavoenzymes;* Muller, F., Ed.; CRC Press: Boca Raton, FL, 1991; Vol. 2, p 437.
(3) Zeller, E. *Classification and Nomenclature of Monoamine Oxidase and Other Amine Oxidases: Structure, Function and Altered Functions;* Academic Press: New York. 1979.
(4) Wouters, J. Structural aspects of monoamine oxidase and its reversible inhibition. *Curr. Med. Chem*. **1998**, *5*, 137−162.
(5) Yamada, M.; Yasuhara, H. Clinical pharmacology of MAO inhibitors: Safety and future. *Neurotoxicology* **2004**, *25*, 11−20.
(6) Rudorfer, M. V.; Potter, V. Z. Antidepressants. A comparative review of the clinical pharmacology and therapeutic use of the "newer" versus the "older" drugs. *Drugs* **1989**, *37*, 713−738.
(7) Gerlach, M.; Double, K.; Reichmann, H.; Riederer, P. Arguments for the use of dopamine receptor agonists in clinical and preclinical Parkinson's diseases. *J. Neural Transm. Suppl.* **2003**, 167−193.
(8) Riederer, P.; Danielczyk, W.; Grunblatt, E. Monoamine oxidase-B inhibition in Alzheimer's desease. *Neurotoxicology* **2004**, *25*, 271−277.
(9) Cesura, A. M.; Pletscher, A. The new generation of monoamine oxidase inhibitors. *Prog. Drug Res*. **1992**, *38*, 171−297.
(10) Youdim, M. B. The advent of selective monoamine oxidase A inhibitor antidepressants devoid of the cheese reaction. *Acta Psychiatr. Scand. Suppl*. **1995**, *386*, 5−7.
(11) Edmondson, D. E.; Mattevi, A.; Binda, C.; Li, M.; Hubalek, F. Structure and mechanism of monoamine oxidase. *Curr. Med. Chem.* **2004**, *11*, 1983−1993.
(12) Carrieri, A.; Carotti, A.; Barreca, M. L.; Altomare, C. Binding models of reversible inhibitors to type-B monoamine oxidase. *J. Comput. Aid.- Mol. Des.* **2002**, *16*, 769−778.
(13) De Colibus, L.; Li, M.; Binda, C.; Lustig, A.; Edmondson, D. E.; Mattevi, A. Three-dimensional structure of human monoamine oxidase A (MAO-A): Relation to the structures of rat MAO-A and human MAO B. *Proc. Natl. Acad. Sci*. **2005**, *102*, 12684−12689.
(14) Binda, C.; Hubalek, F.; Li, M.; Herzig, Y.; Sterling, J.; Edmondson, D. E.; Mattevi, A. Crystal structures of monoamine oxidase B in complex with four inhibitors of the *N*-propargylaminoindane class. *J. Med. Chem.* **2004**, *47*, 1767−1774.
(15) Mevedev, A. E.; Veselovsky, A. V.; Shvedov, V. I.; Tikhonova, T. A.; Moskvitinia, T. A.; Fedotova, O. A.; Axenova, L. N.; Kamyshanskaya, A. Z.; Kirkel, A. Z. and Ivanov, A. Inhibition of monoamino oxidase by pirlindole analogues: 3D-QSAR and CoMFA analysis. *J. Chem. Inf. Comput. Sci*. **1998**, *38*, 1137−1144.
(16) Nunez, M. B.; Maguna, F. P.; Okulik, N. B.; Castro, E. A. QSAR modeling of the MAO inhibitory activity of xanthone derivatives. *Bioorg. Med. Chem. Lett.* **2004**, *14*, 5611−5617.
(17) Todeschini, R and Consonni, V. *Handbook of Molecular Descriptors;* Wiley VCH: Weinheim, Germany, 2000.
(18) Kier, L. B.; Hall, L. H. *Topological Indices and Related Descriptors in QSAR and QSPR;* Gordon and Breach Science Publishers: Amsterdam, 1999; pp 445−489.
(19) Estrada E.; Uriarte, E. Recent advances on the role of topological indices in drug design discovery research. *Curr. Med. Chem.* **2001**, *8*, 1573−1588.
(20) Estrada, E.; Uriarte, E.; Montero, A.; Teijeira, M.; Santana, L.; De Clercq, E. A novel approach for the virtual screening and rational design of anticancer compounds. *J. Med. Chem.* **2000**, *43*, 1975−85.
(21) Karelson, M.; Lobanov, V. S.; Katritzky, A. R. Quantum-chemical descriptors in QSAR/QSPR studies. *Chem. Rev.* **1996**, *96*, 1027−1043.
(22) Bultinck, P.; Langenaeker, W.; Carbo-Dorca, R.; Tollenaere, J. P. Fast calculation of quantum chemical molecular descriptors from the electronegativity equalization methodology. *J. Chem. Inf. Comput. Sci.* **2003**, *43*, 422−428.
(23) Sanderson, R. T. Electronegativity and bond energy. *J. Am. Chem. Soc.* **1983**, *105*, 2259−2261.
(24) Mortier, W. J.; Ghosh, S. K.; Shankar, S. Electronegativity-equalization method for the calculation of atomic charges in molecules. *J. Am. Chem. Soc*. **1986**, *108*, 4315−4320.
(25) Freund, J. A.; Poschel, T., Eds. Stochastic processes in physics, chemistry, and biology. In *Lecture Notes in Physics;* Springer-Verlag: Berlin, Germany. 2000.
(26) González-Díaz, H.; Agüero, G.; Cabrera, M. A.; Molina, R.; Santana, L.; Uriarte, E.; Delogu, G.; Castañedo, N. Unified Markov thermodynamics based on stochastic forms to classify drugs considering molecular structure, partition system, and biologic species. Distribution of the antimicrobial G1 on rat tissues. *Bioorg. Med. Chem. Lett*. **2005**, *15*, 551−557.
(27) González-Díaz, H.; Cruz-Monteagudo, M.; Molina, R.; Tenorio, E.; Uriarte, E. Predicting multiple drugs side effects with a general drug-target interaction thermodynamic Markov model. *Bioorg. Med. Chem.* **2005**, *13*, 1119−1129.
(28) González-Díaz, H.; Torres-Gómez, L. A.; Guevara, Y.; Almeida, M. S.; Molina, R.; Castañedo, N.; Santana, L.; Uriarte, E. Markovian chemicals "*in silico*" design (MARCH-INSIDE), a promising approach for computer-aided molecular design III: 2.5D indices for the discovery of antibacterials. *J. Mol. Mod.* **2005**, *11*, 116−123.
(29) Van Waterbeemd, H. Discriminant analysis for activity prediction. In *Chemometric Methods in Molecular Design. Method and Principles in Medicinal Chemistry*; Manhnhold, R., Krogsgaard-Larsen, P., Timmerman, H., Eds.; VCH: Weinhiem, 1995; Vol. 2, pp 265−282.
(30) Kleeman, A.; Engel, J.; Kutscher, B.; Reichert, D. *Pharmaceutical Substances*, 4th ed.; George Thieme Verlag: Stuttgart, 2001.
(31) Negwer, M. *Organic Chemical Drugs and Their Synonyms;* Akademie-Verlag: Berlin, 1987.
(32) Santana, L.; Uriarte, E.; Roleira, F.; Mihazes, N.; Borges, F. Furocoumarins in medicinal chemistry. Synthesis, natural occurrence and biological activity. *Curr. Med. Chem*. **2004**, *11*, 3239−3261.
(33) Gnerre, C.; Catto, M.; Francesco, L.; Weber, P.; Carrupt, P.-A.; Altomare, C.; Carotti, A.; Testa, B. Inhibition of monoamine oxidase by functionalized coumarin derivatives: Biological activities, QSAR, and 3D-QSARs. *J. Med. Chem*. **2000**, *43*, 4747−4758.
(34) Chimenti, F.; Secci, D.; Bolasco, A.; Chimenti, P.; Granese, A.; Befani, O.; Turini, P.; Alcaro, S.; Ortuso, F. Inhibition of monoamine oxidases by coumarin-3-acyl derivatives: Biological activity and computational study. *Bioorg. Med. Chem. Lett*. **2004**, *14*, 3697−3703.

(35) Antonello, C.; Marciani-Magno, S.; Gia, O.; Carlassare, F.; Baccichetti, F.; Bordin, F. Diethylaminoalkyloxycoumarin and -furocoumarin derivatives. *Il Farmaco, Ed. Sci.* **1979**, *34*, 139−156.
(36) Hansen, J. B.; Bjerring, P.; Buchardt, O.; Ebbesen, P.; Kanstrup, A.; Karup, G.; Knudsen, P. H.; Nielsen, P. E.; Norden, B.; Ygge, B. Psoralenamines. 3. Synthesis, pharmacological behavior, and DNA binding of 5-(aminomethyl)-8-methoxy-, 5-[[(3-aminopropyl)oxy] methyl]- and 8-[(3-aminopropyl)oxy]psoralen derivatives. *J. Med. Chem.* **1985**, *28*, 1001−1010.
(37) Nakamura, Y. Photocrosslinking and the cleavage of DNA by iron complex-substituted psoralen. *Chem. Lett.* **1989**, *1*, 51−54.
(38) Gia, O.; Tonconi, M. T.; Uriarte, E. Benzo and tetrahydrobenzofurocoumarins: New potential photochemotherapeutic drugs. *Il Farmaco* **1997**, *52*, 289−294.
(39) Corda, L. Delogu, G.; Favretto, D.; Maccioni, E. Podda, G.; Santana, L.; Tomaselli, P.; Traldi, P.; Uriarte, E. Synthesis and mass spectrometric investigation of some new coumarin derivatives. *Rapid. Comm. Mass Spectrom.* **1998**, *12*, 2041−2046.
(40) Dalla Via, L.; Gia, O.; Viola, G.; Bertoloni, G.; Santana, L.; Uriarte, E. Photobiological studies of new cyclopentenepsoralens. *Il Farmaco* **1998**, *12*, 638−644.
(41) Terán, C.; Miranda, R.; Santana, L.; Teijeira, M.; Uriarte, E. Synthesis of angular and linear benzofurocoumarins. *Synthesis* **1997**, *12*, 1384−1386.
(42) Dalla Via, L.; Gia, O.; Marciani-Magno, S.; Teijeira, M.; Santana, L.; Uriarte, E. New tetracyclic analogues of photochemotherapeutic drugs 5-MOP and 8-MOP: Synthesis, DNA interacction and antiproliferative activity. *J. Med. Chem.* **1999**, *42*, 4405−4413.
(43) Rodighiero, G.; Antonello, C. Sintesi di alcuni derivati 3-amminocumarinici e prime notizie sulle loro propietà antibatteriche. *Bolletino Chim. Farm.* **1958**, *97*, 592−601.
(44) Antonello, C.; Marciani-Magno, S.; Baessato, O.; Palumbo, M. 3-Amino- and 3-oxy-derivatives of psoralen: Preparation and interactions with DNA. *Il Farmaco, Ed. Sci.* **1981**, *36*, 565−584.
(45) Méndez-Álvarez, E.; Soto-Otero, R.; Sánchez-Sellero, I.; López-Rivadulla, L. M. Inhibiton of brain monoamine oxidase by adducts of 1,2,3,4-tetrahiisoquinoline with components of cigarette smoke. *Life Sci.* **1997**, *60*, 1719−1727.
(46) Méndez-Álvarez, E.; Soto-Otero, R.; Sánchez-Sellero, I.; López-Rivadulla, L. M. *In vitro* inhibition of catalase activity by cigarette smoke: Relevance for oxidative stress. *J. Appl. Toxicol.* **1998**, *18*, 443−448.

JM0509849